American Mineralogist, Volume 76, pages 1940–1949, 1991

Pt-Fe alloys in experimental petrology applied to high-pressure research on Fe-bearing systems

Sieger R. van der Laan,* A. F. Koster van Groos
Department of Geological Sciences, University of Illinois at Chicago, Chicago, Illinois 60680, U.S.A.

Abstract

A double capsule technique is described of Pt-Fe alloy inserts in Pt capsules aimed at eliminating Fe loss in high-pressure experiments. Alloy compositions in equilibrium with a silicate melt are calculated following Grove's (1981) approach, which has been extended to include the effect of pressure. The experimental lifetime of the double capsule is limited because of Fe diffusion from the alloy insert to the Pt outer capsule; it is mainly dependent on thickness of the insert and the temperature of the experiment. Pressure causes a small decrease in diffusivity. The lifetime expectancy of the double capsule assembly is given for various temperatures, and it is compatible with the commonly chosen duration of the experiments. The Pt-Fe alloy controls the $(a_{FeO})^3/(a_{Fe_2O_3})$ and f_{O_2} of the sample through the exchange of Fe^0. For anhydrous samples, an absolute change in the percentage of Fe^{3+} of Fe_{tot} (Fe^{3+}/Fe_{tot}) is associated with a relative change of half that percentage of Fe content of the sample. Hydrous, Fe-bearing samples require the application of an external equilibrium f_{H_2} in addition to the use of Pt-Fe alloys. With lower than equilibrium f_{H_2}, the sample gains Fe from the alloy and loses H_2O; with higher than equilibrium f_{H_2}, the sample loses Fe and gains H_2O. Preliminary results from three sets of experiments are presented to illustrate the effectiveness of this technique. Fe losses can occur if samples are not properly contained by the alloy.

Introduction

Progress in phase equilibrium studies of natural compositions at elevated temperatures and pressures has been seriously hindered by problems with Fe loss from the sample to the capsule. Virtually no reliable high-pressure data exist for natural systems at f_{O_2} in the range of FeO/Fe_3O_4–Ni/NiO (WM–NNO). Many solutions to prevent Fe loss have been proposed for studies at 1 atm based on the use of Pt-Fe alloys (e.g., Ford, 1978; Biggar, 1981; Grove, 1981). From these studies, it is clear that Fe loss can be successfully prevented through the use of Pt-Fe-alloy capsule in equilibrium with sample. In this paper we extend the approach of Grove (1981) to high pressures and describe a technique that allows studies in anhydrous and hydrous Fe-bearing systems.

Experimental rationale

Choice of capsule material

A variety of materials has been used to encapsulate experimental samples in high-pressure experiments. Au and Ag are restricted by their low melting points. Metals of the Pt group dissolve significant amounts of Fe. Mo, Fe, and W interfere chemically and require a low oxidation state in the experimental charge (Biggar, 1970; O'Hara, 1976; Visser and Koster van Groos, 1979). Graphite-lined Pt capsules (e.g., Lesher and Walker, 1988; Koyaguchi, 1989) also require reducing conditions. Solid mantle phases have been used as container material in the study of solid-melt assemblages (e.g., Stolper, 1980; Takahashi and Kushiro, 1983; Fujii and Scarfe, 1985), but the saturation of the melt with the container material severely limits the compositional range of study. The obvious approach to overcome Fe loss is to use Fe alloys such as Pt-Fe for capsule material. However, in current techniques the composition of the Pt-Fe alloy has not been based on capsule-sample equilibrium and, therefore, appears inadequate (Ford, 1978; Chen and Lindsley, 1983; Baker and Eggler, 1987).

A general analysis of capsule-sample interaction indicates the potential to use the capsule composition to control the activities of components in the sample. At thermodynamic equilibrium in the capsule-sample system, no net transfer of any component occurs between the capsule and the sample, and the chemical potential of each component is constant throughout the system. In experiments, this leaves the option to use a container material in which the solubility of a component is either so low that a negligible amount needs to be transferred to reach equilibrium concentrations in the capsule material or so high that the capsule forms an infinite reservoir for that component, in which case the chemical potential of the component can be controlled with the capsule composition.

* Present address: Hawaii Institute of Geophysics, University of Hawaii at Manoa, 2525 Correa Road, Honolulu, Hawaii 96822, U.S.A.

0003–004X/91/1112–1940$02.00

When using Pt capsules in Fe-bearing samples in the f_{O_2} range NNO–WM, the sample is dominated by Fe^{2+} and Fe^{3+} species. However, the concurrent very low Fe^0 activity in the sample still requires high equilibrium concentrations of Fe in the capsule material because of the small activity coefficient for Fe^0 in Pt (e.g., Grove, 1981). This behavior is not unique for Fe in Pt but is observed for alloys of many first-series transition elements with Pt-group metals (Hultgren et al., 1973).

Capsule-sample interaction

The capsule-sample equilibrium for Fe involves Fe^0, FeO, Fe_2O_3, and O_2. When controlling a_{Fe} in the Pt-Fe capsule and f_{O_2} in the system at a given P and T, the activities of FeO and Fe_2O_3 are fixed by the reactions

$$Fe + \tfrac{1}{2}O_2 = FeO \quad \text{with} \quad K_1 = a_{FeO}/(a_{Fe}\cdot\sqrt{f_{O_2}}) \quad (1)$$

and

$$Fe + Fe_2O_3 = 3FeO \quad \text{with} \quad K_2 = (a_{FeO})^3/(a_{Fe}\cdot a_{Fe_2O_3}). \quad (2)$$

Because a sealed capsule is closed to O exchange, adjustments of these activities can only be made internally through transfer of Fe between sample and foil. The composition of the alloy and the sample impose a f_{O_2} on the system (Eq. 1), whereas the a_{Fe} of the alloy imposes a specific $(a_{FeO})^3/(a_{Fe_2O_3})$ on the sample (Eq. 2). To reach equilibrium, the Fe exchange between the alloy and sample is generally minor. For example, a melt with 20% Fe^{3+}/Fe_{tot} (Fe^{3+} of Fe_{tot}) at NNO and 10% Fe^{3+}/Fe_{tot} at WM and containing 10 wt% FeO (Fe_{tot} as FeO) will undergo approximately a 0.5 wt% FeO change (Fe_{tot} as FeO) adapting from one f_{O_2} to the other.

Under hydrous conditions f_{O_2} is also affected by

$$H_2O = H_2 + \tfrac{1}{2}O_2 \quad \text{with} \quad K_3 = f_{H_2}\cdot\sqrt{f_{O_2}}/f_{H_2O}. \quad (3)$$

It is well known that capsules are permeable with respect to H_2 (e.g., Shaw, 1963; Hewitt, 1977). This implies that in studies on Fe-bearing hydrous systems both an externally applied f_{H_2} and a fixed a_{Fe} in the capsule are necessary. With knowledge of the equilibrium constant of Equation 3 as a function of P and T, the required f_{H_2} can be readily calculated using appropriate fugacity-composition models (e.g., Holloway, 1987).

Pressure dependence of the alloy-sample equilibrium

Using the f_{O_2} associated with the Fe_2O_3/FeO of a melt (Sack et al., 1980) and including the effect of pressure, we can calculate equilibrium alloy compositions from Equation 1 (cf. Grove, 1981). The f_{O_2} at 1 bar for constant Fe_2O_3/FeO and temperature (T) may be obtained using

$$\ln f_{O_2}\,(P = 1) = [\ln(X_{Fe_2O_3}/X_{FeO}) - b/T - c - d_iX_i]/a \quad (4)$$

where a, b, c, and d_i are constants, and d_iX_i represents the compositional dependence of the f_{O_2} with the Fe_2O_3/FeO ratio of the bulk composition (Sack et al., 1980). The effect of pressure (P) on f_{O_2} can be approximated following Mo et al. (1982) with

$$\ln f_{O_2}\,(\text{at } P) = \ln f_{O_2}\,(P = 1) + (2\bar{v}_{Fe_2O_3} - 4\bar{v}_{FeO})(P - 1)/RT \quad (5)$$

for the pressure range, where $\delta v/\delta P = 0$. The pressure dependence of the equilibrium of Equation 1 may be evaluated from the partial molar volumes of Fe in the alloy and FeO in the melt, $\bar{v}_{Fe}$(alloy) and $\bar{v}_{FeO}$(melt). Assuming that the volume of reaction is independent of P and T in the experimental range, the following expression was obtained:

$$\ln K_1 = -[\Delta G^0(T) + \Delta\bar{v}_T(P - 1)]/RT. \quad (6)$$

Values for $\Delta G^0(T)/(RT)$ are from Grove (1981), and $\Delta\bar{v}_T$ = 4.34 cm³ was derived for T = 1250 °C as follows: For the partial molar volume of Fe^0 in Pt a value $\bar{v}_{Fe}$(alloy) = 7.484 cm³ was obtained from the molar volume of γFe (fcc structure) at 1250 °C (Skinner, 1966), and another value of 7.53 cm³ at 20 °C and 8.47 cm³ at 1250 °C was obtained by extrapolating the cell parameters for Pt-Fe compounds with fcc structure (Cabri and Feather, 1975) to an Fe end-member. An intermediate value $\bar{v}_{Fe}$(alloy) = 8.0 cm³ was adopted, and a value $\bar{v}_{FeO}$(melt) = 12.34 cm³ (1250 °C) (Nelson and Carmichael, 1979) was used. The volume term in Equation 6 is not important. At 1250 °C and 10 kbar, this term contributes less than 3% to the value of ln K. The calculation of the alloy's a_{Fe} is thus dependent on our ability to determine f_{O_2} of the melt properly.

With a value for a_{FeO} and using the calculated f_{O_2} for a bulk composition of known Fe_2O_3/FeO, the a_{Fe}(alloy) can be calculated from Equation 6. We used $a_{FeO} = X_{FeO}$ since Grove (1981) showed that for a diverse range of natural magmas this did not cause a much poorer fit in his regression to derive the constants of Equation 6. Using the activity-composition relation of Heald (1967), the equilibrium alloy composition can be obtained. In this procedure a pressure effect on γ_{Fe} in the alloy has not been taken into account (Gudmundsson and Holloway, 1989). The pertinent numerical values to perform these calculations are summarized in Appendix 1.

Experimental method

Capsule preparation

A double capsule design was developed in which an outer capsule of Pt (wall thickness, 0.1 mm) is lined with a Pt-Fe alloy foil that is 0.025–0.1 mm thick. The thicker foils were used in experiments of longer duration. The foil insert is shorter than the capsule so that only the outer Pt capsule is welded after both the capsule and the foil are crimped shut. The foils are prepared by uniformly electroplating a thin Pt cylinder. The weight gain from plating determines the Pt-Fe ratio of the foil. After plating, the foils are annealed to produce a homogeneous foil. Details of the plating and annealing procedure are described in a manual (van der Laan and van der Laan, unpublished data), which is available upon request. The design is similar to that of Chen and Lindsley (1983), but

TABLE 1. Starting compositions for experiments

Sample	TGI*	Margi* **	Bonin* **	CV-46* **	TT152†
SiO_2	59.66	54.93	58.82	59.34	50.63
TiO_2	0.44	0.51	0.14	0.51	1.88
Al_2O_3	13.57	13.15	11.06	10.62	13.91
Fe_2O_3	0.00	0.00	0.00	0.00	2.27
FeO	6.33	8.20	8.43	9.27	10.20
MgO	9.66	11.52	11.71	12.57	6.56
CaO	6.25	10.21	7.79	5.74	11.42
Na_2O	2.66	1.17	1.61	1.37	2.64
K_2O	1.30	0.26	0.42	0.49	0.17
P_2O_5	0.13	0.04	0.02	0.10	0.21
Total	100.00	99.99	100.00	100.01	99.88

* Prepared as gel.
** Details about compositions are described in van der Laan et al. (1989).
† TT152-21, basalt glass from Juan de Fuca ridge segment 6. Major elements analyzed on the University of Washington ARL-EMS electron probe (J.R. Delaney, unpublished data).

we used a different method of plating and annealing, which resulted in more homogeneous foils.

Starting materials and experimental technique

Three sets of experiments were performed with the starting materials listed in Table 1. The first data set was obtained using three boninite and one sanukitoid composition (Table 2). The experiments were performed in an internally heated pressure vessel (IHPV) (Holloway, 1971), equipped with a double-wound W furnace, that allowed heating rates to 450 °C/min. The pressure medium was Ar. Temperature was controlled to within 3 °C, but a gradient of 25–30 °C was usually observed with respect to a second thermocouple at 8 mm vertical distance. The reported temperatures (Table 2) are averages of the two readings; they are believed precise to within 5 °C because of the constant capsule-thermocouple geometry for all experiments and the reproducibility of the experiments. Pressure, measured using high-precision Heise gauges and a Harwood manganin cell, is accurate to within 1%. The samples were quenched within seconds by turning the vessel vertical, allowing the capsules to drop into the cooler part of the furnace.

The second data set (Table 3) consists of two experiments, JED-2 and JED-3, on a natural basalt glass (Table 1) under H_2O-saturated conditions. They were done in an IHPV of different design (Holloway, unpublished data). Conditions were 1160 ± 30 °C at 310 bars and 1170 ± 30 °C at 520 bars with an external P_{H_2} of 5 and 10 bars, respectively. Duration was 2 h. Details of these experiments will be published elsewhere (Dixon, in preparation).

The third data set (Table 3) consists of a few experiments on the same basalt glass as in set 2, conducted in a ½-in. piston cylinder apparatus using talc assemblies. The experiments were at 1300 ± 10 °C and 10 ± 0.5 kbar nominal pressure (hot piston in) for 6 h.

After the experiments, the capsules were weighed, sectioned, polished, examined microscopically, and analyzed. The first set was analyzed with a JEOL 35CF SEM with Tracor Northern EDS using ZAF data correction for the Pt-Fe alloys (with pure metal standards) and using the Bence and Albee correction (1968) for the silicates (with the common mineral standard set). For the distance measurements of the diffusion profiles, the magnification scale bar was calibrated on a diffraction grating replica. The other experiments were analyzed on a JEOL 733 Superprobe with CIT-ZAF correction. Fe^{3+}/Fe^{2+} was determined for all the glassy products of the second and third set of experiments using wet chemistry (Sack et al., 1980). H_2O contents were determined by FTIR spectros-

TABLE 2. Experimental conditions and results on boninites (data set 1)

Sample	Experiment	Duration (min)	Phases*	P total (kbar)	T (°C)	Wt%** H_2O	FeO-total gain†	Olivine† Forsterite	Olivine† K_d'	% Fe^{3+} (based on K_d)	% Fe^{3+} (calculated)‡	Wt% Fe in Pt§ Start	Wt% Fe in Pt§ End
Margi	31.4	28	L + ol + opx	1.0	1215	3.0	1.5	88.3–88.8	0.267–0.28	6.5–11.0	14.2	6.1	
	25.2	30	L + ol + opx	1.0	1220	1.6	0.8	87.2	0.335		11.5	7.6	
	26.3	30	L + ol + opx	1.0	1240	1.6	1.0	87.7	0.294	2.0	12.7	6.6	
	42.1	26	L(Q) + ol + opx	4.0	1200	4.0	1.3	88.8	0.273	9.1	15–18	5.7	4.8
Bonin	30.4	30	L + ol + opx	1.0	1278	1.0	−0.4	90	0.290	3.4	16–19	5.2	4.4
	46.1	27	L + ol + opx	1.8	1210	4.2	0.3	90.2–91.1	0.234–0.261	13.1–21.9	26.0	3.2	
	46.2	27	L + ol + opx	1.8	1210	4.7	0.4	90.7	0.243	18.9	26.1	3.2	
	47.2	27	L(Q) + ol	3.0	1180	6.1	0.5	90.3–91.2	0.226–0.252	16.0–24.6	22.8	3.8	
	47.3	27	L(Q) + V + ol	3.0	1180	6.6	0.0	90.4–91	0.246–0.264	12.0–18.1	21.3	3.9	
TGI	31.2	28	L + ol	1.0	1215	3.4	1.5	91.6	0.202	32.5	14–17	5.9	5.0
	47.4	27	L + ol	3.0	1180	5.0	0.5	88.0–90.6	0.263–0.345	12.4	20.9	4.1	4.2
	45.1	27	L + ol + opx	3.0	1240	2.2	0.0	89.6–90.9	0.274–0.317	8.8	18.4	4.4	4.4
	49.3	27	L(Q) + ol	7.5	1107	10.9	0.5	90.2–90.9	0.253–0.275	8.3–15.5	21.2	3.9	3.7
CV-46	46.4	27	L + ol + px	1.8	1210	4.9	0.4	89.7–90.0	0.257–0.265	11.6–14. 5	25.5	3.2	
	40.2	27	L(Q) + V + ol + cen	2.0	1181	6.0	2.2	87.2–89.1	0.238–0.286	4.7–20.6	16–21	5.3	3.9
	40.3	27	L + V + ol + cen	2.0	1181	7.1	1.5	87.1–89.4	0.246–0.307	18.0	15–16	5.6	5.2

* L = liquid; Q = quench crystals; V = vapor; ol = olivine; opx = enstatite; cen = clinoenstatite; px = ortho- and clinoenstatite.
** Estimated error: less than ±0.5 wt%.
† Error margins discussed in text.
‡ Range is calculated with start and end alloy compositions.
§ Error: ±0.2 wt%.

TABLE 3. Experimental conditions and results on basalt glass (data sets 2 and 3)

Sample	Experiment	Duration (h)	P total (kbar)	T (°C)	Wt% H_2O* Start	Wt% H_2O* End	FeO total change	Measured** % Fe^{3+}	Measured** FeO	Measured** Fe_2O_3	Calculated % Fe^{3+}†	Calculated FeO	Calculated Fe_2O_3	Wt% Fe in Pt‡ Start	Wt% Fe in Pt‡ End
TT152	JED-2	2	0.31	1160	0.36	1	−0.5	17.9	9.6	2.33	19–21	9.34	2.66	6.5	6.5
	JED-3	2	0.52	1170	0.36	1.4	−0.4	21.5	9.26	2.82	20–22	9.33	2.77	6.1	6.1
	JdF-1	6	10	1300	0.36	n.d.	−4.4	5.7	7.35	0.5	6.1	7.67	0.55	11.7	10.4
	JdF-3	6	10	1300	0.36	n.d.	−4.8	14.6	6.32	1.2	6.1	7.3	0.53	9.7	10
	JdF-5	6	10	1300	0.36	1.7	−6.2	10.5	5.37	0.7	6.7	5.97	0.48	6.6	9.1
	JdF-6	6	10	1300	0.36	2.1	−1.8	1.7	10.22	0.2	5.5	10.01	0.65	14.5	11.8
	JdF-7	6	10	1300	0.36	2.1	−2.5	12.3	8.5	1.33	12.9	8.66	1.43	4.7	6

* Error: less than 10%.
** Relative error is 5% in % Fe^{3+} in JED experiments (cf. Christie et al., 1986); other errors discussed in text.
† Range in values is obtained with minimum and maximum temperature of the experiment (see text).
‡ Error: less than 0.2 wt%.

copy using the molar absorption coefficients of Dixon et al. (1988).

Results and discussion

Lifetime of the capsule assembly

A concentration step exists between the Pt-Fe foil and the Pt capsule, causing Fe to diffuse across the foil-capsule interface during the course of an experiment (Fig. 1). Eventually Fe at the foil-sample interface will be affected, which limits the foil's effective life span.

The temperature dependency of Fe diffusion in Pt at 1 atm and at 1100–1400 °C was determined by Berger and Schwartz (1978). Data concerning the pressure dependency were not available and have been determined from the first set of experiments—those on boninite compositions (van der Laan et al., 1989). In these experiments, temperatures were usually reached within 15 min and in less than 3 min after reaching 900 °C. Experiments were carried out between 1100 and 1300 °C at 1 kbar to 7.5 kbar and accurately timed durations were between 25 and 30 min. The Fe concentration profile was measured with SEM-EDS on a cross section perpendicular to the interface.

Concentration gradients never developed over more than 20 μm on each side of the interface, much less than the foil or capsule thickness. A value for the Fe-diffusion coefficient was derived from the profile by regressing the data to fit the solution of Fick's second law for diffusion between two semi-infinite media (Shewmon, 1963). The diffusion coefficient was assumed to be independent of composition in the Fe range studied, 3.2–7.6 wt%. The concentration profile across the interface is described by

$$C(d,t) = \tfrac{1}{2}C_0[1 - \mathrm{erf}(z)] \quad (7)$$

where C_0 = initial concentration of Fe in foil, d = distance from the interface, $z = d/\sqrt{(4Dt)}$, D = the diffusion coefficient, and t = time. The value of z is determined by rearranging Equation 7 and then taking the inverse error function of the concentration term $1 - 2C(d,t)/C_0$. Values for D were obtained by plotting d against z. Diffusion coefficients thus obtained were pressure and temperature specific. Multiple profiles were measured on a single sample, and average diffusion coefficients for each sample are reported in Table 4.

A multiple linear regression of $\ln(D)$ vs. $1/T$ and $(P - 1)/T$ yielded the pressure and temperature dependence of the diffusion coefficient (Shewmon, 1963) of

$$D = D_0\, e^{-(Q/RT) - \Delta V(P-1)/RT} \quad (8)$$

A weighting factor was applied to the averaged D-values based on the observed temperature gradient during the experiment. This factor was calculated as $100/\Delta T$.

Our values for D_0, Q, and ΔV together with the values of Berger and Schwartz (1978) are presented in Table 5, and our values with the extrapolated 1 bar and 10 kbar diffusivities are shown in Figure 2. The slightly higher D values found in our study compared with those of Berger and Schwartz are attributed to diffusion of Fe during the heating stage before the temperature of the experiment was attained. The activation volume of diffusion (ΔV = 3.26 ± 0.98 cm³/mol) contributes a small decrease in D with pressure. It needs mentioning, however, that the P and T conditions of the experiments roughly correlate; experiments at higher P are generally conducted at lower

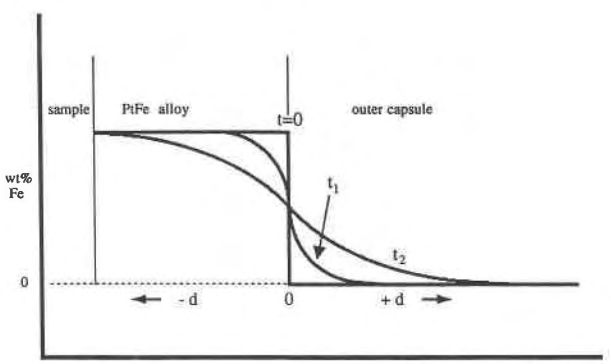

Fig. 1. Progressive homogenization through Fe diffusion across the interface between the foil and outer capsule as described by Equation 7. Eventually the Fe content at the foil-sample interface will be affected.

TABLE 4. Results of the Fe diffusion measurements

Experiment	P (kbar)	T (°C)	ΔT	D (10^{-10} cm²/s)	1σ D	R^2	1σ R^2	No.	N	1σ N
27	1	1273	10	1.659	0.232	0.973	0.037	4	7.5	0.3
29	1	1265	45	2.888	0.370	0.987	0.005	4	12.25	3.6
30	1	1274	17	3.192	0.906	0.994	0.001	2	9.5	1.0
31	1	1210	15	0.976	0.113	0.993	0.005	3	8.33	0.6
33	3	1262	14	3.237	0.441	0.990	0.007	3	11.33	2.1
34	7	1270	16	1.801	0.128	0.991	0.005	4	9.5	1.3
35	7	1241	8	1.377	0.179	0.994	0.003	5	7.2	1.8
37	7	1207	17	0.832	0.130	0.989	0.010	3	7.67	2.3
40	2	1181	12	0.721	0.138	0.990	0.007	3	9.33	3.8
41	4	1225	13	0.992		0.996		1	14	
42	4	1200	12	0.779	0.068	0.996	0.003	6	5.67	2.6
45	3	1240	16	1.378	0.093	0.994	0.002	4	10.75	1.3
47	3	1180	13	0.509	0.036	0.991	0.004	3	7.67	1.2
49	7.5	1107	15	0.182	0.017	0.990	0.014	6	5.83	1.3

Note: P = pressure; T = temperature and range (ΔT); D = per experiment averaged diffusivity in cm²/s and the standard error in its mean value (1σ D); R^2 = mean R^2 of goodness of fit and its standard deviation (1σ R^2); No. = number of profiles contributing to the average; N = average amount of points per profile and the standard deviation in the average number of points contributing (1σ N).

T. As an artifact of this correlation, Q and ΔV obtained by regression become correlated which introduces additional uncertainties in their values.

Based on our 1-bar diffusion coefficients (highest mobility), a conservative estimate for the lifetime of these foils was calculated as a function of thickness and the rate of diffusion at the temperature of the experiment:

$$t_d = d^2/(4Dz^2) \tag{9}$$

where d represents the thickness of the foil and z is the argument of the error function erf(z). Values of z were obtained by calculating the erf(z) corresponding to changing values of C/C_0. In Equation 7 a value of erf(z) = 1 corresponds to no change in foil composition. It is also noted that doubling the foil thickness results in a fourfold increase in the lifetime of the foil. Figure 3 shows the lifetime of a foil 0.1 mm thick ($t_{0.1\text{mm}}$) as a function of temperature. This figure can be used to estimate the potential lifetime (t_d) of any foil of thickness d (in millimeters) since

$$t_d = (d/0.1)^2 \cdot t_{0.1\text{mm}}. \tag{10}$$

This expression is strictly valid only for an alloy adjacent to the sample that still has its original composition, that is, for a semi-infinite couple geometry.

Changes in sample composition

Our experiments were not designed to test this double capsule technique, and they are complicated by hydrous conditions. The experiments demonstrate the intricacies of multiple redox equilibria and the importance of H_2 buffering for hydrous samples. Three cases emerge: (1) Fe content of a sample increasing without H_2 buffering, (2) Fe content remaining constant under equilibrium external f_{H_2}, and (3) Fe content decreasing with higher than equilibrium external f_{H_2}. The presence of H_2O in the capsule and the transport of H_2 through the capsule wall indirectly create an additional O_2 source or sink; e.g., reduction of FeO or Fe_2O_3 is accommodated by formation of H_2O, whereas values of f_{O_2} remain in agreement with the alloy-sample equilibrium. Mass balance for O_2 should be maintained as long as O_2 is not transferred across the capsule wall. In order to calculate the O_2 mass balance, H_2O contents have to be accurately known before and after an experiment. Compositional parameters of all experiments are listed together with the experimental conditions in Tables 2 and 3.

Boninite experiments

In the first set of experiments on boninite-H_2O, no external H_2 pressure was applied, and short durations of 25–30 min were chosen to reduce H_2 loss. Temperatures were at near-liquidus conditions. Loss of H_2 (and thus H_2O) continuously increased f_{O_2} during the experiment. The glasses of the products are heterogeneous with respect to Fe, and values represent averages, with Fe_{tot} as FeO varying by as much as ±0.7 wt% FeO. Most samples gained Fe, but the exchange of Fe was minor: in nine out of 16 experiments less or equal 0.5 wt% FeO, in six between 0.8 and 1.5 wt%, and in one 2.2 wt%.

In the experiments a decrease in alloy Fe content is accompanied by an increase in Fe_{tot} (as FeO) of the melt.

TABLE 5. D_0 and the parameters Q and ΔV for the P and T dependence of Fe diffusion in Pt

D_0 (cm²/s)	Q (kJ/mol)	ΔV (cm³/mol)	
0.50 (+0.49/−0.25)	275 (±8.4)	3.26 (±1.0)	this study
2.5 (+1.6/−0.9) 10^{-2}	243.4 (±6.3)		Berger and Schwartz (1978)

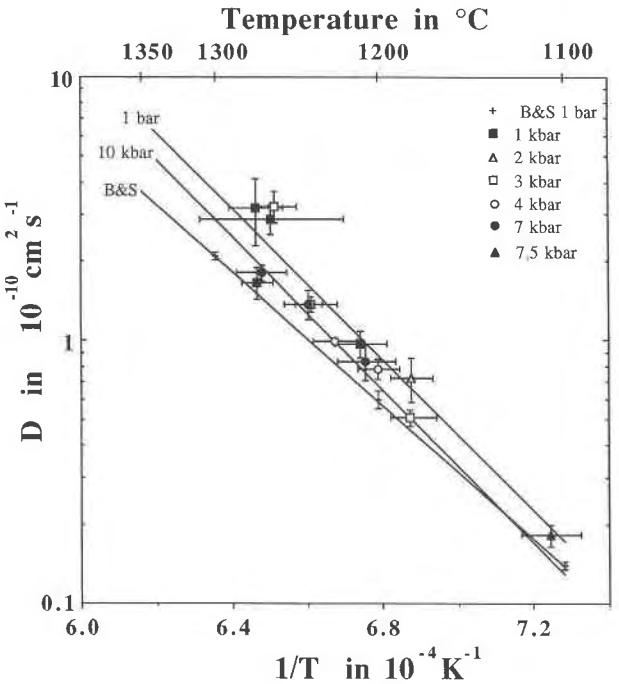

Fig. 2. Diffusion coefficients for Fe in Pt from this study compared with those of Berger and Schwartz (1978). For each experiment, an average D with 1σ-error margins and ΔT range is plotted. Lines represent best fits to our data, extrapolated to 1 bar and 10 kbar, and to the 1-bar data (marked B&S) of Berger and Schwartz (1978).

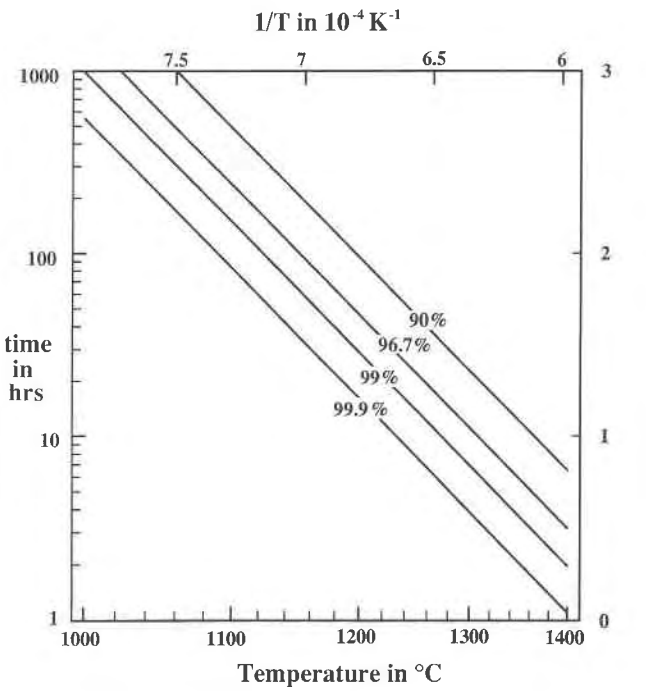

Fig. 3. Lifetime of a double capsule with a 0.1 mm Pt-Fe foil insert as function of temperature calculated using our 1-bar diffusion coefficient. Isopleths are for the remaining percentage of fe in the foil at the interface with the sample.

Alloys with high Fe content (>5 wt%) result in a larger Fe gain by the sample and have larger Fe losses from the foil except in experiment Bonin 30.4 (Table 2).

The Fe^{3+}/Fe_{tot} of the products of crystals + melt was determined by comparison of

$$K_d' = (Fe^{2+}/Mg)_{ol}/(Fe_{tot}/Mg)_{melt} \quad (11)$$

to the Roeder and Emslie (1970) value $K_d = 0.3$ for

$$K_d = (Fe^{2+}/Mg)_{ol}/(Fe^{2+}/Mg)_{melt}. \quad (12)$$

the ratio K_d'/K_d gives the Fe^{2+}/Fe_{tot} in the melt. Some K_d' values are larger than $K_d = 0.3$ and cannot be applied to estimate the Fe^{3+}/Fe_{tot} of the melt (experiments 25.2, 47.4, 45.1). Such high K_d' values could often be related to opaque inclusions in olivines.

The effective initial oxidation state of the starting material was $Fe^{2+}/Fe_{tot} = 100\%$. Oxidation of Fe^{2+} to Fe^{3+} generally resulted in Fe^{3+}/Fe_{tot} below 20%. Experiments with low H_2O contents, i.e., experiments 30.4, 26.3, and 45.1, developed the lowest Fe^{3+}/Fe_{tot} because of minor H_2 loss as a result of a small H_2 gradient between the inside and outside of the capsule. All except one experiment (31.2) stayed below the calculated alloy equilibrium value of Fe^{3+}/Fe_{tot}. Loss of Fe from the sample in order to attain Fe^{3+}/Fe_{tot} values in equilibrium with the alloy was expected but not observed. The most likely reason for the lower than equilibrium values of Fe^{3+}/Fe_{tot} of the melts is that the rims of olivine are actually higher in Fo than the analyzed spots. Olivine rim compositions are difficult to determine because of overlap contamination with the surrounding glass in the analyses. A change in forsterite content from Fo_{89} to Fo_{91} will mean a relative decrease of 20% in the Fe^{2+} fraction of the melt (e.g., $Fe^{2+}/Fe_{tot} = 90\%$ with $Fe^{3+}/Fe_{tot} = 10\%$ will become $Fe^{2+}/Fe_{tot} = 72\%$ and $Fe^{3+}/Fe_{tot} = 28\%$). It appears that Fe^{3+}/Fe_{tot} values of Table 2 lie largely within the range of error. The observations therefore agree with the expected buffering of Fe^{3+}-Fe^{2+} by the alloy. The Fe^0 of the alloy enters the melt to maintain the alloy-melt equilibrium for the Fe species.

Experiments at controlled f_{H_2} on basalt glass

The two experiments with an externally imposed f_{H_2}, JED-2 and JED-3 (Table 3), were done at H_2O-saturated conditions. The H_2O content of the glass products was analyzed using FTIR spectroscopy, and the observed variation in H_2O content of ± 0.2 wt% is attributed to quench effects.

The melts have a slightly lower Fe content than an earlier analysis of the starting composition (Delaney, unpublished data). This could reflect compositional variation in the starting material, because a difference of 1 wt% was also observed in CaO content, or capsule-sample Fe exchange. In JED-2, if Fe exchange with the alloy had occurred, vigorous convection must have homogenized the melt. In JED-3, heterogeneities in Fe_{tot} (as FeO) of

±0.3 wt% are larger than the analytical error and probably point to some alloy-sample exchange. However, the unchanged alloy compositions and only slightly, if at all, changed melt compositions appear to indicate equilibrium for the Fe reaction.

The f_{O_2} was controlled with an external f_{H_2} at QFM. Based on the expression of Sack et al. (1980), Fe^{3+}/Fe_{tot} percentages of 13.2–13.3 were expected at QFM; however, measured values were 17.9 and 21.5. Our calculations based on alloy composition, Fe_{tot} of the melt, and the alloy controling $(a_{FeO})^3/(a_{Fe_2O_3})$ (Eq. 2) of the melt give Fe^{3+}/Fe_{tot} of 19–21% and 20–22%, which is in better agreement with the respective measured values. The f_{O_2} must therefore have been close to (QFM + 1.3) ± 0.5 log f_{O_2} units (or NNO + 0.4) for p_{H_2O} = 310 and 520 bar and for p_{H_2} = 5 and 10 bar. Alternatively, capsule, sample, Fe^{3+}/Fe_{tot}, and f_{O_2} were in equilibrium at QFM during the experiments, and Fe^{3+}/Fe_{tot} changed upon quench and fortuitously matched our calculation.

Piston-cylinder experiments on basalt glass

In all these experiments, which were carried out at 10 kbar, Fe is lost from the sample. The Fe concentration of the alloy at the foil-sample interface converges at about 10 wt%. Alloys with lower than 10 wt% initial Fe^0 showed a maximum Fe content at the sample-alloy interface. Alloys with higher than 10 wt% Fe had a maximum in their Fe profiles but had lower value than their initial alloy composition. In these experiments Fe contents in the alloy dropped both toward the sample as well as the outer capsule, indicating an Fe flux in both directions. The observed Fe loss from the sample is therefore attributed to loss via direct sample-outer capsule pathways and not to exceeded lifetime of the double capsule. Note that this does not contradict our theory since the alloy only controls $(a_{FeO})^3/(a_{Fe_2O_3})$ (Eq. 2) and not the absolute amounts.

Measured values of Fe^{3+}/Fe_{tot} range from 1.7 to 14.6%. In cases where the alloy had a maximum in its profile, indicating Fe supply to the sample, Fe^{3+}/Fe_{tot} is exceedingly low (5.7% and 1.7%). In the experiments where the alloy gained Fe, Fe^{3+}/Fe_{tot} is 10.5%, 12.3%, and 14.6%. In Figure 4, we plotted calculated percentage Fe^{3+}/Fe_{tot} isopleths as a function of f_{O_2} and pressure for Juan de Fuca basalt at 1300 °C as well as the isopleths for equilibrium alloy compositions. Using the range of alloy composition from start to end of the experiments, three of the five experimental Fe^{3+}/Fe_{tot} ratios lie within the alloy-sample equilibrium range. Experiments that deviate from this range are JdF-3, with measured Fe^{3+}/Fe_{tot} of 14.6% and calculated equilibrium value of 6.1–6.4%, and JdF-6, with 1.7% measured and 4.1–5.5% calculated.

In addition to Fe loss, H_2O gain of 1.5–1.8 wt% occurred in the experiments. The piston-cylinder assembly imposes a f_{H_2} on the sample because of talc-graphite reactions, but the value is unknown because of thermal gradients over the graphite heater. The H_2 diffuses through the capsule and reduces Fe oxides of the sample to form

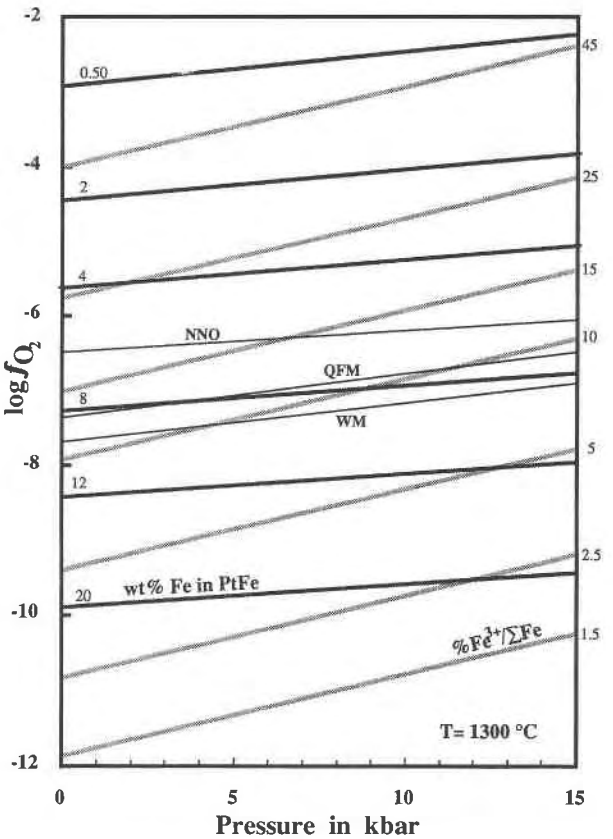

Fig. 4. Calculated equilibria for Pt-Fe alloys and Juan de Fuca basalt TT152-21 as a function of pressure and f_{O_2} at 1300 °C. Isopleths for Fe^{3+}/Fe_{tot} percentages are marked on the right and for wt% Fe in Pt on the left. The figure is valid only for the exact bulk composition of Table 1, and isopleth positions will change with Fe exchange. Oxygen fugacity buffers NNO, QFM, and WM are according to Huebner (1971).

H_2O. In a system only open to H_2 exchange, loss of 1.0 wt% FeO corresponds to a 0.25 wt% H_2O gain by mass balance. However, H_2O gain after the experiment (Table 3) is not in agreement with the Fe losses and FeO and Fe_2O_3 contents in JdF-6 and JdF-7. An excess of at least 1 wt% H_2O is unaccounted for, and an additional source of O needs to be invoked.

In the experiments, the Fe loss of the sample is highly variable (Table 3). Wet chemical analyses to determine Fe^{3+}/Fe^{2+} contents are not necessarily more accurate than the olivine-K_d method applied in set 1 when dealing with heterogeneous Fe distribution. The observation that Fe was lost from all samples does indicate a possible heterogeneity in Fe content. Because the Fe^{2+} content was determined on bulk sample and Fe_{tot} was determined from spot analyses, errors in Fe^{3+} content may result as Fe^{3+} is determined by difference.

Some deviation is to be expected in our experiments for reasons other than lack of agreement between pre-

dicted and observed Fe^{3+}/Fe_{tot}. The discrepancy can be partly attributed to inaccuracies in calculating the alloy composition. Because our alloy calculations are based on Grove's (1981) measurements at 1 atm, it is necessary to assess the error margins of that study. Grove's data (see Grove, 1981, Fig. 5) show a spread about the calculated vs. observed a_{Fe} one-to-one relation, with calculated alloy compositions being generally within 10% of the measured values. The Fe^{3+}/Fe^{2+} contents in Grove's study were calculated rather than measured for the temperature and f_{O_2} conditions of the experiments using the relationship of Sack et al. (1980). Difficulties in predicting alloy compositions must therefore be attributed to the effect of bulk composition on the activities of Fe species and the approximate predictive quality of the empirical calibration by Sack et al., because identical alloy compositions could be readily produced starting with both high-Fe and Fe-free Pt in Grove's experiments. Christie et al. (1986) reported an uncertainty of ± 0.5 $\log_{10}$ units in f_{O_2} value in the experimental calibration of Sack et al. Figure 4 can be used to evaluate the effect of these uncertainties on alloy and melt composition.

O mass balance

In our experiments at 10 kbar, the sample is open to H_2 and Fe^0 exchange. The O_2 released by Fe oxide reduction reacts with H_2 resulting in increased H_2O contents. Based on O_2 mass balance, it appears that approximately 1 wt% excess H_2O is present in experiments JdF-6 and JdF-7. This H_2O gain requires an additional source for the H_2O in the capsule. No obvious source could be identified. The alloys used in the experiments showed no signs of surface oxidation after annealing. Glass cylinders of the starting material rather than powder were used to minimize the effect of adhered H_2O, and air contained in the capsule was insufficient to explain the large excess H_2O gain. It is possible that recrystallization of the Pt and Pt-Fe alloys created permeability for O_2 or H_2O along grain boundaries and that contamination occurred during the experiments. An alternative source for O could be the reduction reaction of silica to form Si-Pt alloy as was observed by Chen and Presnall (1975). This would imply very reducing conditions for the piston-cylinder experiments. We have not analyzed alloys for Si. There is some evidence of problems with O_2 mass balance in experiments by other workers, but an unexplained loss rather than a gain of O_2 seems to be the case. In Chen and Lindsley's (1983) experiments using Pt-Fe alloy capsules, progressive Fe losses from the samples were reported with time. Thoroughly dried BN assemblies were used, and no source of H_2 could be invoked. They concluded that FeO reacts to form Fe metal and Fe_2O_3. Although they did observe blebs of metallic Fe, they did not substantiate the presence of large amounts of Fe_2O_3 nor the absence of H_2O in their products. Mysen and Virgo (1978) argued that released O from Fe^{3+} reduction in their experiments on melts in the system acmite-jadeite dissolved into the melt. In both experiments, loss of O_2 from the capsule would also explain the observations.

The effect of pressure on Fe^{3+}-Fe^{2+} speciation

The effect of pressure on the $2FeO + \frac{1}{2}O_2 = Fe_2O_3$ equilibrium is expressed by the volume of reaction term. A change in activity coefficients with pressure cannot be evaluated with the existing data. The large positive value at 1 atm for $\bar{v}_{Fe_2O_3} - 2\bar{v}_{FeO}$ implies a preference for Fe^{2+} at elevated pressures, but a change from fourfold to sixfold coordination of Fe^{3+} could drastically reduce the partial molar volume of Fe_2O_3. No such coordination change was found by Luth and Brearley (1989) in basalt glass quenched from 20 kbar pressure. Kress and Carmichael (1989) reported that $\bar{v}_{Fe_2O_3} - 2\bar{v}_{FeO}$ remains positive and is approximately independent of pressure to greater than 40 kbar based on the isothermal compressibilities for FeO and Fe_2O_3 derived from acoustic velocity measurements. Based on these studies, very low Fe^{3+}/Fe^{2+} would be expected in f_{O_2}-buffered melts at high pressure. Indeed, such results were reported by Luth and Brearley (1989), and the Fe^{3+}/Fe^{2+} ratios agreed with predictions based on the volume of reaction. However Gudmundsson et al. (1988) presented contradictory experimental results and concluded that the pressure effect on Fe^{3+}/Fe^{2+} is either nonexistent or causes a slight increase in this ratio.

In our experiments, Fe^{3+}/Fe_{tot} percentages calculated for the capsule-melt equilibrium agree reasonably well with the observed values at elevated pressure. The large error margin in experimental Fe^{3+}/Fe_{tot} values precludes definitive conclusions from the current data sets, but it seems that the pressure effect on Fe^{3+}-Fe^{2+} speciation is appropriately predicted by the volume term in Equation 5 for the equilibrium constant.

Summary

The use of alloy capsules and the control of a_{Fe} requires a conceptually different view of experimental systems. If a capsule is closed with respect to O, a change in oxidation state of Fe^{3+}/Fe^{2+} can only be accomplished in the presence of other internal O_2 sources or sinks. In the following overview, we attempt to develop systematically the redox conditions under various commonly enacted experimental conditions in Fe-bearing systems.

Closed system involving one redox equilibrium only. An example would be the redox equilibrium $2FeO + \frac{1}{2}O_2 = Fe_2O_3$. Closed-system conditions only exist with inert, nonalloying capsules and in the absence of other O_2 sources or sinks in a sample such as C-CO_2, H_2-H_2O, or S-SO_2. In this case, although an isothermal increase in pressure will change f_{O_2} drastically, Fe^{3+}/Fe^{2+} will not change since increase in f_{O_2} involves reduction of negligible amounts of Fe^{3+}. The isothermal P-f_{O_2} path can be illustrated using Figure 4 where sample compositions would stay on isopleths of Fe^{3+}/Fe_{tot}.

Closed system involving two redox equilibria. One example is $2FeO + \frac{1}{2}O_2 = Fe_2O_3$ and $Fe^0_{caps.} + \frac{1}{2}O_2 = FeO$.

In this case, a_{Fe} is practically fixed by the reservoir size of the alloying capsule (assuming γ_{Fe} independent of pressure). With an isothermal increase in pressure, Fe^{3+}/Fe_{tot} of a sample will follow or stay close to the Fe^0 isopleth as, e.g., in Figure 4. Other examples would be $2FeO + \frac{1}{2}O_2 = Fe_2O_3$ and a metal–metal oxide buffer such as NNO or WM (Huebner, 1971) in an inert capsule or a sample contained in a graphite container. In these cases Fe^{3+}/Fe_{tot} of a sample will follow the f_{O_2} of the buffering reaction. (See Fig. 4 for examples.) With graphite in a sealed Pt capsule, the sample will follow the CCO buffer only when a free CO-gas phase is present.

Closed or open system involving multiple (more than 2) equilibria. Examples would include redox equilibria: $2FeO + \frac{1}{2}O_2 = Fe_2O_3$, $Fe^0 + \frac{1}{2}O_2 = FeO$, and $H_2 + \frac{1}{2}O_2 = H_2O$. In this case, it is essential that f_{H_2} and a_{Fe} imply the same f_{O_2} in their respective equilibria, or large changes in the sample in H_2O and FeO/Fe_2O_3 contents will result. This is illustrated by the results of our three sets of experiments. It should also be clear that the use of Fe-free alloying capsules with disequilibrium external f_{H_2} (buffered or from talc in a piston-cylinder assembly) will lead to highly suspect experimental results in Fe-bearing samples.

Carmichael and Ghiorso (1986) extensively discussed internal redox equilibria in ascending magmas, touching on many of the same problems evaluated in this paper. From our deliberations it should be clear that the outcome of experimental investigations of Fe^{3+}/Fe^{2+} equilibria is entirely dependent on the experimental approach.

Acknowledgments

We are very much indebted to K.C. van der Laan for setting up an Fe-plating facility adapted to our special needs. T.L. Grove is thanked for reviewing an earlier version of this manuscript, and Victor Kress and Laurinda Chamberlin are thanked for their critical comments on this version. We are grateful to J.R. Delaney and Veronique Robigou-Nelson for supplying basalt glass, to Jackie Eaby Dixon for sharing experimental results, and to I.S.E. Carmichael for providing ferric-ferrous analyses. P.J. Wyllie generously made available his experimental facilities for piston-cylinder experiments. Support from the NSF grant EAR-8212738 is acknowledged.

References cited

Baker, D.R., and Eggler, D.H. (1987) Compositions of anhydrous and hydrous melts coexisting with plagioclase, augite, and olivine or low-Ca pyroxene from 1 atm to 8 kbar: Application to the Aleutian volcanic center of Atka. American Mineralogist, 72, 12–28.

Bence, A.E., and Albee, A.L. (1968) Empirical correction factors for the electron micro-analysis of silicates and oxides. Journal of Geology, 76, 382–403.

Berger D., and Schwartz, K. (1978) Zur Fremddiffusion in Platin. Neue Huette, 23, 210–212.

Biggar, G.M. (1970) Molybdenum as a container for melts containing iron-oxide. Bulletin of the American Ceramic Society, 49, 286–288.

——(1981) Melting experiments on ocelli and matrix samples from proterozoic lavas in South Africa. Bulletin Minéralogique, 104, 369–374.

Cabri, L.J., and Feather, C.E. (1975) Platinum-iron alloys: A nomenclature based on a study of natural and synthetic alloys. Canadian Mineralogist, 13, 117–126.

Carmichael, I.S.E., and Ghiorso, M.S. (1986) Oxidation-reduction relations in basic magma: A case for homogeneous equilibria. Earth and Planetary Science Letters, 78, 200–210.

Chen, C.-H., and Presnall, D.C. (1975) The system Mg_2SiO_4-SiO_2 at pressures up to 25 kilobars. American Mineralogist, 60, 398–406.

Chen, H.-K., and Lindsley, D.H. (1983) Apollo 14 very low titanium glasses: Melting experiments in iron-platinum alloy capsules. Proceedings of the 14th Lunar Planetary Science conference. Journal of Geophysical Research, 88 (suppl. B), 335–342.

Christie, D.M., Carmichael, I.S.E., and Langmuir, C.H. (1986) Oxidation state of mid-ocean ridge basalt glasses. Earth and Planetary Science Letters, 79, 397–411.

Dixon, J.E., Stolper, E., and Delaney, J.R., (1988) Infrared spectroscopic measurements of CO_2 and H_2O in Juan de Fuca Ridge basaltic glasses. Earth and Planetary Science Letters, 90, 87–104.

Ford, C.E. (1978) Platinum-iron alloy sample containers for melting experiments on iron-bearing rocks, mineral and related systems. Mineralogical Magazine, 42, 271–275.

Fujii, T., and Scarfe, C.M. (1985) Composition of liquids coexisting with spinel lherzolite at 10 kbar and the genesis of MORBs. Contributions to Mineralogy and Petrology, 90, 18–28.

Grove, T.L. (1981) Use of FePt alloys to eliminate the iron loss problem in 1 atmosphere gas mixing experiments: Theoretical and practical considerations. Contributions to Mineralogy and Petrology, 78, 298–304.

Gudmundsson, G., and Holloway, J.R. (1989) The activity coefficient of iron in platinum at 1400 °C and from 1 atm to 20 kbar. Eos, 70, 1402.

Gudmundsson, G., Holloway, J.R., and Carmichael, I.S.E. (1988) Pressure effect on the ferric/ferrous ratio in basaltic liquids. Eos, 69, 1511.

Heald, E.F. (1967) Thermodynamics of iron-platinum alloys. Transactions of the Metallurgical Society of AIME, 239, 1337–1340.

Hewitt, D.A. (1977) Hydrogen fugacities in Shaw bomb experiments. Contributions to Mineralogy and Petrology, 65, 165–169.

Holloway, J.R. (1971) Internally heated pressure vessels. In G.C. Ulmer, Ed., Research techniques for high pressure and high temperature. Springer-Verlag, New York.

——(1987) Igneous fluids. In Mineralogical Society of America Reviews in Mineralogy, 17, 211–234.

Huebner, J.S., (1971) Buffering techniques for hydrostatic systems at elevated pressures. In G.C. Ulmer, Ed., Research techniques for high pressure and high temperature. Springer-Verlag, New York.

Hultgren, R., Desai, P.D., Hawkins, D.T., Gleider, M., and Kelley, K.K. (1973) Selected values of the thermodynamic properties of binary alloys. American Society for Metals, Metals Park, Ohio.

Koyaguchi, T. (1989) Chemical gradient at diffusive interfaces in magma chambers. Contributions to Mineralogy and Petrology, 103, 143–152.

Kress, V.C., and Carmichael, I.S.E. (1989) Compressibilities of Fe_2O_3 in silicate melts and the redox evolution of ascending magmas. Eos, 70, 1402.

Lesher, C.E., and Walker, D. (1988) Cumulate maturation and melt migration in a temperature gradient. Journal of Geophysical Research, 93, 10295–10311.

Luth, R.W., and Brearley, M. (1989) Iron in basaltic magmas at high pressure. Eos, 70, 1402.

Mo, X., Carmichael, I.S.E., Rivers, M., and Stebbins, J. (1982) The partial molar volume of Fe_2O_3 in multicomponent silicate liquids and the pressure dependence of oxygen fugacity in magmas. Mineralogical Magazine, 45, 237–245.

Mysen, B.O., and Virgo, D. (1978) Influence of pressure, temperature, and bulk composition on melt structures in the system $NaAlSi_2O_6$-$NaFe^{3+}Si_2O_6$. American Journal of Science, 278, 1307–1322.

Nelson, S.A., and Carmichael, I.S.E. (1979) Partial molar volumes of oxide components in silicate liquids. Contributions to Mineralogy and Petrology, 71, 117–124.

O'Hara, M.J. (1976) Control of charge composition during experiments on "dry" basalts. Progress in experimental petrology, vol. 3, p. 136–140. National Energy Research Council, London.

Roeder, P.L., and Emslie, R.F. (1970) Olivine-liquid equilibrium. Contributions to Mineralogy and Petrology, 29, 275–289.

Sack, R.O., Carmichael, I.S.E., Rivers, M., and Ghiorso, M.S. (1980) Ferric-Ferrous equilibria in natural silicate liquids at 1 bar. Contributions to Mineralogy and Petrology, 75, 369–376.

Shaw, H.R. (1963) Hydrogen-water vapor mixtures: Control of hydrothermal atmospheres by hydrogen osmosis. Science, 139, 1220–1222.

Shewmon, P.G. (1963) Diffusion in solids. McGraw-Hill, New York.

Skinner, B.J. (1966) Thermal expansion. Geological Society of America Memoirs 97, 75–96.

Stolper, E. (1980) A phase diagram for mid-ocean ridge basalts: Preliminary results and implications for petrogenesis. Contributions to Mineralogy and Petrology, 74, 13–27.

Takahashi, E., and Kushiro, I. (1983) Melting of a dry peridotite at high pressures and basalt magma genesis. American Mineralogist, 68, 859–879.

van der Laan, S.R., Flower, M.F.J., and Koster van Groos, A.F. (1989) Experimental evidence for the origin of boninites: Near-liquidus phase equilibria between 1 and 7.5 kbar. In A. Crawford, Ed., Boninites and related rocks. Unwin Hymann, London.

Visser, W., and Koster van Groos, A.F. (1979) Phase relations in the system K_2O-FeO-Al_2O_3-SiO_2 at 1 atmosphere with special emphasis on low temperature liquid immiscibility. American Journal of Science, 279, 70–91.

Manuscript received July 3, 1990
Manuscript accepted June 26, 1991

Appendix 1. Numerical equivalents of expressions in the text

$$\ln f_{O_2} = [\ln(X_{Fe_2O_3}/X_{FeO}) - b/T - c - \sum d_i X_i]/a \quad (4)$$

where $a = 0.21813$, $b = 13184.7$, $c = -4.4933$, $d_{SiO_2} = -2.15036$, $d_{Al_2O_3} = -8.35163$, $d_{FeO} = -4.49508$, $d_{MgO} = -5.43639$, $d_{CaO} = 0.073113$, $d_{Na_2O} = 3.54148$, $d_{K_2O} = 4.18688$. X_i's are mole fractions of oxides, Fe_{tot} = FeO, and T is in K and P in bars (Sack et al., 1980).

$$\ln f_{O_2} \text{ (at } P \text{ bar)} = \ln f_{O_2} (P = 1) + (0.52126/T - 8.126 \cdot 10^{-5})(P - 1) \quad (5)$$

with T in K and P in bars (Mo et al., 1982).

$$\ln K = -1.187 + 20727/T - 0.0522(P - 1)/T \quad (6)$$

with T in K and P in bars where $K = a_{FeO}^{melt}/(a_{Fe}^{Pt} \cdot \sqrt{f_{O_2}})$ (Grove, 1981; this study). Heald's (1967) activity-composition relation for Fe in Pt:

$$\ln \gamma_{Fe} = (1 - X_{Fe})^2[-3.326564 + 0.221051(4X_{Fe} - 1)].$$

$$D = 0.50\, e^{-33073/T - 0.039(P-1)/T} \quad (8)$$

with T in K and P in bars.